nature climate change

SUPPLEMENTARY INFORMATION

DOI: 10.1038/NCLIMATE1101

Methane emissions from permafrost thaw lakes limited by lake drainage.

This supplementary information includes additional information on thaw lake formation processes, diagrams and tables accompanying the description of the model, model parameters, model testing and experiments, and the calculation of CH4 emission due to thaw lake expansion.

Section S 1 discusses the thaw lake processes that are simulated by the model.
Section S 2 provides additional information to the model description.
Section S 3 contains data on the areas on which the model was tested.
Section S 4 describes the estimation of parameters for the model.
Section S 5 describes the model validation and sensitivity experiments.
Section S 6 describes results of the model experiments .
Section S 7 contains the calculation of CH_4 emission that can be attributed to thaw lake development.

Nclimate1101-s2.avi

This file contains a movie of model output of 2500 years of a model run similar to the terrain experiment. The movie shows the development of lake area and partially thawed grid cells in time steps of 10 years.

The unzipped movie file has a size of 169 MB.

Nclimate1101-s3.zip

This file contains the model source code (C++), a compiled binary file for Mac OS, and example input files. The source code excludes the libraries StochasticLib and NetCDF. In the ReadMe.txt file included in the zip file is indicated where these can be obtained.

This version of the model source code is added in April 2011. For more recent versions of the model contact the first author.

Supplementary information 'Methane emission from permafrost thaw lakes limited by lake drainage.'

J. van Huissteden[1]* C. Berrittella[1]
F.J.W. Parmentier[1,2] Y. Mi[1] T.C. Maximov[3]
A.J. Dolman[1]

April 7, 2011

[1]Vrije Universiteit, Faculty of Earth and Life Sciences, Hydrology and Geo-Environmental Sciences, De Boelelaan 1085, 1081HV Amsterdam, The Netherlands, ko.van.huissteden@geo.falw.vu.nl

[2]Lund University, Department of Earth and Ecosystem Sciences, Physical Geography and Ecosystem Analysis, Sölvegatan 12, 223 62 Lund, Frans-Jan.Parmentier@nateko.lu.se

[3]Russian Academy of Sciences, Siberian Branch, Institute for Biological Problems of the Cryolithozone, 41 Lenin Ave., 677980 Yakutsk, Russia

Contents

The supplementary information includes additional information on thaw lake formation processes, diagrams and tables accompanying the description of the model, model parameters, model testing and experiments, and the calculation of CH_4 emission due to thaw lake expansion.

S 1 discusses the thaw lake processes that are simulated by the model.
S 2 provides additional information to the model description.
S 3 contains data on the areas on which the model was tested.
S 4 describes the estimation of parameters for the model.

S 5 describes the model validation and sensitivity experiments.
S 6 describes results of the model experiments .
S 7 contains the calculation of CH_4 emission that can be attributed to thaw lake development.

S 1. Thaw lake processes.

Thaw lake formation is initiated by climate change (increased precipitation, snow cover, temperature) or anthropogenic and natural processes altering the soil heat balance (e.g. destruction of vegetation cover by human activities, wildfires, natural erosion). Thawing starts preferentially at ice-rich spots such as the ice wedges in arctic polygonal soils[1,2,3,4,5,6]. Besides higher air temperatures, increased snow cover thickness[4] and precipitation[5,7] also initiate thawing. The initial thawing is caused by a relative soil temperature change causing an increase of thaw depth[6]. Once a water-filled depression is formed, thaw of ground ice is enhanced[2,8]. Alternatively, lakes may have been formed by water accumulation in pre-existing depressions after precipitation increase[8]. When the water depth is larger than the maximum winter ice thickness, lakes do not freeze to the bottom and development of thawed permafrost (talik) beneath the lake occurs[9,10]. The development of an unfrozen layer tends to shield the underlying permafrost from further rapid thaw[2].

Lakes expand laterally by thermal and mechanical erosion driven by waves and wind-driven surface currents[1,9] or thaw slumping[11]. Shoreline erosion rates are highest along larger, deeper lakes and in fine-grained, ice-rich deposits[8]. High summer water tables contribute to more rapid lake expansion, which indicates a relation between lake expansion and precipitation next to temperature[12]. Thaw depth is related approximately to the square root of time since development, and lakes expand more rapidly and grow deeper in permafrost with high ice content[13]. Lake formation does not imply complete thaw of permafrost; below a lake frozen material may persist as is the case in continuous permafrost areas. In some areas, thaw lakes are elongated with orientation of the length axis roughly perpendicular to the prevailing summer wind direction, caused by the development of wind-driven circulation cells[14,15]. Lakes may ultimately disappear by drainage through unfrozen sediment, erosion establishing contact with rivers and other lakes[1,14,12,16,17] or infilling with sediment[8,18,19,20]. Lake drainage by erosion is facilitated by

high water tables in both rivers and lakes, and by warm summers[17,20,21]. Partial drainage, with subsequent infilling of shallow remnant ponds with organic deposits and ice wedge growth is common[8]. Currently formation of new lakes occurs in northern parts of the Siberian permafrost area, coinciding with their disappearance in more southerly areas, the latter suggesting drainage through thawed subsoil[16]. Although radiocarbon dating clearly shows that rapid thaw lake expansion was associated with climate warming at the Last Glacial Termination (LGT)[23], the relation of lake change rate to climate change is still poorly quantified.

Several references contain data on pond initiation and lake bank retreat rates (section S4), but this information is rarely quantitatively related to climate change. The shape of the relations between morphological change and climate change is likewise unknown from empirical observations. In our model we have assumed linear relations by default. The physics of permafrost thaw is well known and has been applied in various models. However, the associated morphological changes - pool formation, lake expansion and lake drainage - are usually the result of an array of processes of which thawing of frozen ground is only one[13,24]. E.g. lake bank retreat is a combination of thaw, erosion processes and sediment redistribution; in pond formation also vegetation dynamics may play a role. As a result, it is difficult to obtain well defined relations from physical considerations only. A physics-based model of lake expansion[24] suggests in one of the studied cases a nonlinear relation between mean annual air temperature (MAAT) deviation from a reference climate to the lake expansion rate; the radial expansion accelerates with higher MAAT. In another case this nonlinearity is less clear. The authors of this model also note a large spatial variability in this relation resulting from variations in ground ice content, and a large temporal variability. Therefore assumptions on the exact nature of this relation remain speculative, and a simple linear relation serves in our model as a conservative estimate.

Besides temperature, permafrost thaw and lake change processes are influenced by precipitation. Snow cover influences permafrost thaw, spring flooding and lake levels, and summer precipitation enhances erosion processes on lake banks. Therefore we have included both temperature and precipitation as climate drivers in our model. Quantification of the relation precipitation change - lake change is even more difficult because of scarcity of data. For this reason we resort also here to linear relations and simple threshold values in our model.

We assume that lake development is driven by climatic deviation from a

reference climate at which ice-rich permafrost is geomorphologically stable. An alternative assumption could be that the rate of climate change is the main driver. This is contradicted by the continuing and repeated thaw lake formation during the relatively stable Holocene (see below). On the other hand, the dependence on deviations from a reference climate has been suggested by observations and models[6,24]. Models indicate that lakes do not expand when present MAAT is decreased to glacial levels[24]. The choice of the Last Glacial Maximum climate as reference climate for our study site is further corroborated by the absence of thaw lake deposits in terrestrial sediments of that ages[25].

The concept of a thaw lake cycle has been described by several authors[1,8,9,22]. This autocyclic process of formation and drainage of lakes may mask enhancement of lake formation by climate change. After lake drainage or infilling, new ice-rich permafrost can be established with formation of ice wedges and ice lenses in the sediment, resulting in frost heave. Initial ice wedge width growth in drained thaw lake basins (DTLB's) may be as rapid as 3 cm/year[21]. Re-establishment of large amounts of ground ice subsequently can be followed by renewed lake formation[6,9,22]. Repeated lake formation and drainage can cause large areas to be covered by overlapping DTLB's[9,17]. Regrowth of ground ice and frost heave preferentially occurs in fine-grained deposits in the centers of DTLB's. Ice aggradation may raise the basin surface level to nearly that of the surrounding older terrain[8]. However, the processes involved in the thaw lake cycle may have been too slow for completion of a full cycle during the Holocene[8], in particular in coarser grained deposits which tend to develop less excess ice. In Alaska, long-term lake changes are masked by high short-term variability of lake area[12].

S 2. Additional information to the model description.

The model equations are included in the 'Methods' section of the printed paper. Included here are two block diagrams depicting the model structure. Figure S1 summarizes the thaw lake initialization process in the model, Figure S2 the thaw lake cycle. Table S1 contains a list of the model parameters, and the parameter values used in the simulations. Table S2 contains the model state variables. The model has been coded in C++. It

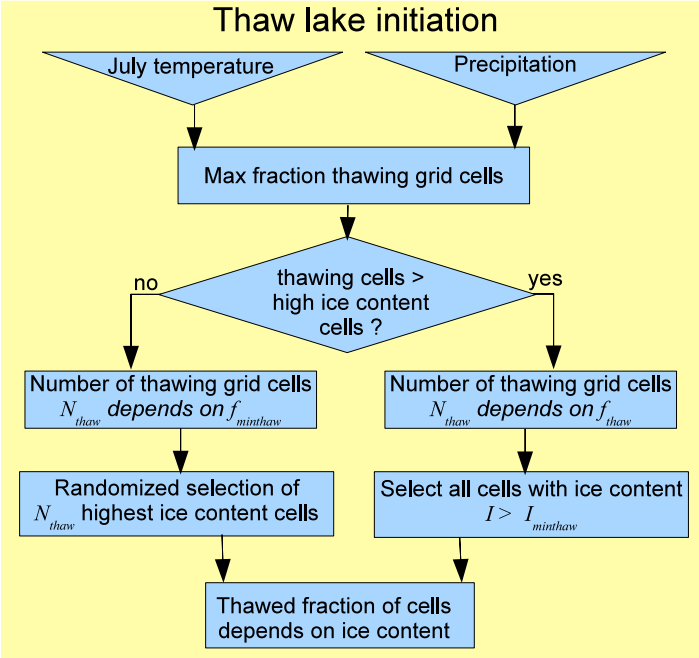

Figure S1. Block diagram of the thaw lake initialization process in the model. The symbols refer to the equations in the Methods section and Table S1 and S2.

includes the random number library StochasticLib, written by Agner Fog, www.agner.org/random. The model source code is made available on the Journal's web site; for a recent version, contact the first author.

The model assumes flat terrain, underlain by ice-rich permafrost. In the description of the model, 'thawed area' refers to model grid cells which consist partially or completely of open water (thaw ponds or lake). We denote thaw here as surficial thaw causing subsidence and pond or lake formation, not the complete disappearance of permafrost. 'Lakes' are clusters of completely thawed grid cells. 'Drained area' are lakes that have been added to the drainage system, and potentially may refreeze depending on temperature conditions.

The model grid consists of 500 x 500 = 250,000 cells. We used a grid cell size of 40 x 40 m; this is sufficient for covering small lakes in the area with 2 or more grid cells. We experimented also with a grid cell size of 20

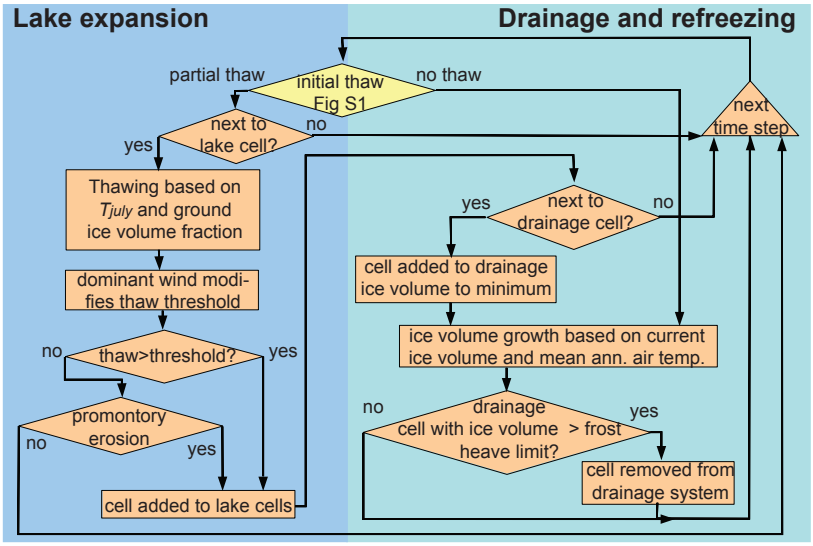

Figure S2. Block diagram of thaw lake drainage and ground ice regrowth. The symbols refer to the equations in the Methods section and Table S1 and S2.

x 20 m, and found no difference in model behavior. Parameters that have to be adjusted to the grid cell size are L_{max} for lake initiation and the lake expansion parameters b and c. The initial conditions of the model consist of prescribed permafrost ice content for each grid cell. A normally distributed random component is added. An initial drainage system is prescribed by indicating which grid cells are part of a river floodplain. Optionally, existing lakes can be prescribed.

Symbol	Description	Units	Range	TERRAIN
I_{min}	Minimum volumetric ice content		0.3-0.5	0.3
I_{max}	Maximum volumetric ice content		0.6-0.9	0.8
$I_{minthaw}$	Minimum ice content for initiation of thawing			0.6
$T_{ref,july}$	Reference July temperature	^oC		7
$T_{ref,ann}$	Reference mean annual air temperature	^oC	< 0	-17.5
P_{ref}	Reference precipitation	mm		140
M_T	Constant relating max. fraction of thawing cells f_{thaw} to summer temperature deviation $T_{diff,t}$	$^oC^{-1}$		2.0e-6
M_P	Constant relating max. fraction of thawing cells f_{thaw} to precipitation deviation $P_{diff,t}$	mm^{-1}		2.0e-6
L_{max}	Max. fraction of cells thawed per time step			0.5
L_{thresh}	Threshold thaw fraction above which a cell completely thaws		< 1	0.5
a	Temperature offset in relation lake expansion L_{maxexp} to july temperature dev. $T_{diff,t}$	$^oC^{-1}$	5-0	-1
b	Const. rel. lake expansion - july T dev. $T_{diff,t}$	$^oC^{-1}$		0.000875
c	Const. rel. lake expansion - precip. dev. $P_{diff,t}$	mm^{-1}		2.0e-4
W	Dominant wind direction	^{o}	$0 - 360^o$	315
F_w	Weight factor for wind orientation		1-4	1
L_{drain}	Threshold thaw fraction for drainage		0.4-0.8	0.6
M_{drain}	Reduces L_{drain} depending on precipitation	mm^{-1}		0.004
T_{freeze}	Upper temperature limit for permafrost in cells	^oC	$< -1^o$	-1
T_{grow}	Upper temperature limit for ice growth in cells	^oC	$< -5^o$	-7
I_{grow}	Ice content growth factor in non-thawed cells		< 0.002	5.0e-3
I_{heave}	Ice content above which frost heave occurs			0.35
G	Grid cell width	m	25-100	40
P_t	Annual precipitation	mm		
$T_{july,t}$	Mean July temperature	^oC		
$T_{ann,t}$	Mean annual air temperature	^oC		

Table S1. Model parameters and input. Symbol: symbols used in model equations; Range: value range if appropriate. The column TERRAIN shows the parameters for the TERRAIN and FUTURE experiments (S 5).

Symbol	Description	Units	Range
i	Grid cell row index		
j	Grid cell column index		
N	Number of grid cells		
t	Time (discrete time steps)	year	
$I_{i,j,t}$	Grid cell volumetric ice content at time t		$0 - I_{max}$
$T_{diff,t}$	Summer temperature deviation $T_{july,t} - T_{ref,july}$	^oC	
$P_{diff,t}$	Precipitation deviation $P_t - P_{ref}$	mm	
$f_{thaw,t}$	Maximum fraction of grid cells where thaw is initiated		0-1
$f_{minthaw,t}$	Fraction of grid cells of which the ice content exceeds the minimum ice content for thawing $I_{minthaw}$		0-1
$N_{thaw,t}$	Number of grid cells where thawing is initiated at time t		
p_{erode}	Erosion probability for promontory cells		0-1
$L_{i,j,t}$	Area fraction of cell which consists of thaw ponds at time t		0-1
$L_{new,i,j,t}$	Area fraction of grid cell where new thaw ponds are established		0-1
L_{dir}	Threshold area fraction above which the grid cell completely thaws in case of wind direction sensitive lake expansion		0-1
$L_{exp,i,j,t}$	Area fraction of cell affected by thaw lake expansion		
$L_{drain,t}$	Drainage threshold corrected for precipitation	mm^{-1}	
G	Orientation of a grid cell with respect to grid cell at index i, j	^{o}	

Table S2. Model state variables. Symbol: symbols used in model equations; Range: value range if appropriate.

S 3. Test area.

The Indigirka Lowlands (IL) test area is situated north of the Berelegh river, in an area that is covered by remnants of ice-rich Pleistocene permafrost ('yedoma') and DTLB's. To the north of the area, a number of very large lakes occurs. The area is centered on the Kytalyk tundra research station (70° 48' N, 147° 26' E)[26,27]. MAAT and July temperature of the nearby (30 km) Chokurdagh airport weather station are -14.3°C and 9.5°C respectively (years 1961-1990). Since approximately 1980 the temperature has increased with warming concentrated in the summer and autumn months. The average July temperature over the years 1980-2010 increased with 0.053°C yr $^{-1}$. Annual precipitation amounts 232±58 mm, range 113-356 mm (years 1966-2008). Most precipitation (58%) falls in the months May-September, about half

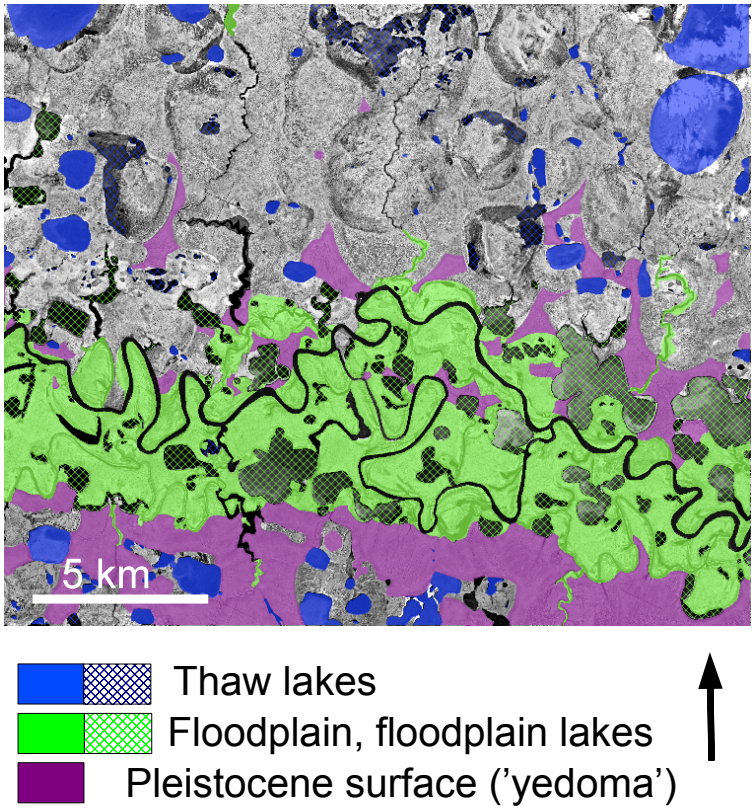

Figure S3. Model test area. Satellite image and digitized thaw lakes near the Kytalyk research station, Indigirka Lowlands area (IL), Northeast Siberia.

of the precipitation falls as snow. Snow cover thickness did not increase significantly (1980-2010). The wind directions in the area are dominated slightly by northwesterly winds.

	Kytalyk, Indigirka Lowlands (IL)
Location center	N70°50', E147°29'
Area	559.6 km^2
Geology	Pleistocene-Holocenene fluvial silt, clay, loess
Permafrost	Continuous, ice-rich permafrost ground ice in ice lenses, ice wedges, pingos, palsas
Remote sensing data	KH9-13 image 1977/07/09; 7.9 m resolution GeoEye-1 image 2010, 0.5 m resolution
Present climate	T_{ann} -14.3°C, T_{july} 9.5°C, P 232 mm
Last Glacial climate	T_{ann}-17.5°C, T_{july} 6.5°C, P 140 mm
Dominant wind dir.	315°

Table S3. Geographical and climate data including paleoclimate and present climate of the test area. Kytalyk is a research station for tundra and permafrost carbon cycle research[26]. The Last Glacial reference climate has been derived from paleobotanical data[32].

Near the research station, thaw lake expansion rates in ice-rich permafrost have been determined by comparing satellite images of different dates (KH9 military reconnaissance satellite image dating from 1977, with 7.9 m resolution, GeoEye-1 image from 2010, 0.5 m resolution). A lake close to the station expanded on average 0.19 m yr^{-1} into an approximately 15 m high ice-rich permafrost plateau. Also the number of ponds created by thawing of palsas and ice wedges in the area has increased. However, the spatial resolution of the KH9 image does not allow areal quantification of these ponds. The KH9 image has been used to map the existing lakes over an area of the same size as the model area. The KH9 image excludes the most recent thaw features that might have been generated by recent climate warming (Fig. S3). We used only lakes that are not connected to the river for comparison, lakes connected to the river would be classified by the model as 'drained' and generally have a strongly varying water table and lake area throughout the year. The area is covered by a wet to mesic tundra vegetation, consisting of a mosaic of sedge meadows, *Sphagnum*, *Betula nana* patches. Methane fluxes are measured in a typical tundra vegetation in a DTLB.

S 4. Model parameter values.

Systematic observation data relating thaw lake initiation and expansion to climate change are absent and have to be extracted from widely scattered literature. In the Alaskan coastal plain a 3.8% increase of thaw ponds or 1200 pits/km^2 is associated with a 2-5°C warming of the mean annual ground temperature, attributed to warmer summers and higher precipitation between 1989 and 1998, starting in particular with extreme weather in 1989 (43% higher thawing degree day sum, 60% higher precipitation)[6]. This amounts to a precipitation increase of ±43 mm and summer temperature increase of 2.9°C (assuming a 100 day thawing season). This would result in maximal values for M_T of 0.013 °C^{-1} and M_P of 0.0009 mm^{-1}. However, these values should be considerably lower when combined in our model.

In Central Yakutia, a lake expansion rate of 0.8-4 m yr^{-1} is observed[2] with a modest summer warming of approximately 0.5°C and an increase in T_{ann} of 2.4°C due to rising winter temperatures[5,28,29]. If this occurs at a lake bank bordering a grid cell of 40 x 40 m, then a fraction of 0.01 - 0.05 of the grid cell area is consumed by lake expansion each year at a sustained summer warming of 1°C (b parameter in eq. 7, Methods). However, the cited expansion rates are instantaneous values over possibly short sections. The expansion of one lake measured in our study area would result in a value of b of 0.0876 °C^{-1}. This value is possibly an overestimate due to specific local conditions; a survey over a larger area is in progress. We suspect that several lake expansion rates cited in literature focus on extreme values, and clearly the establishment of a database of observations will enhance reliability of model parameters. In the model simulations presented below, lower values on thaw pond initiation and lake expansion had to be used to obtain realistic results (Table S1). Above a certain limit of thawing, the amount of water in a grid cell should enhance further thawing[6]. The threshold above which a grid cell is considered as completely thawed L_{thresh} is set at 0.5.

The maximum ice volume fraction of the IL area is set at 0.8. We observed frequent massive ground ice and very large ice wedges in river bank exposures. The ice content determined on a network of small core samples in a DTLB in the IL area ranged between 40% and 90%. In similar Alaska coastal plain areas an ice volume fraction of 0.9 has been observed[12]. The mean annual air temperature limit for establishment of new permafrost is set to -1°C, the limit for significant regrowth of ground ice (ice wedges) at -7°C being a frequently cited temperature limit for ice wedge formation[30,31]. In our test

area ground ice growth by pingo and palsa formation, which may occur at higher temperatures[31], also occurs but is restricted in area.

Parameters for lake drainage are likewise difficult to estimate. In the model a threshold thaw fraction is assumed, above which grid cells can be connected to the drainages system (L_{drain}). Observations show that drainage occurs when lake expansion or river meandering brings lakes into contact with each other or the drainage system[12,17] and is enhanced at higher lake levels due to high precipitation. We assume a value of L_{drain} of 0.6 and consider it reduced to 0 with an annual precipitation excess P_{diff} of 15 mm. As yet, no significant subsurface drainage through the active layer and taliks is included in the model. The temperature limits of our simulations stay below a MAAT of -7°C, at which continuous permafrost is sustained.

S 5. Model validation and sensitivity experiments.

Here we describe the model experiments to test the performance and sensitivity of the model and to quantify past and future lake development.

TERRAIN : These experiments are used for model testing against observed lake distributions in the test area and to test simulated system dynamics on longer time scales. Parameter values are set as indicated in section S4 and Table S1. The experiments simulate lake development during the LGT and Holocene. The configuration of the drainage system is hypothetical. The ground ice volume fraction is assumed to be homogeneous throughout the area, with superposed random variation. We used an ensemble of 10 model runs. Three additional model runs have been analyzed in more detail to compare the spatial properties of the generated lakes with those of the terrain. Additional experiments have been included to check the effects of assuming a different drainage system configuration with a lower drainage density and inhomogeneous ground ice distribution (Fig. S4) The inhomogeneous ground ice distribution is generated by allocating segments of the grid with varying average ground ice volume fraction and superposed random variation. The time series of climate change consists of an increase of temperatures and precipitation with 80% of the difference Glacial-Holocene (Table S3) in 100 years, followed by a gradual increase to full Holocene values

in 1000 years. The simulations for the past climate lasts 8000 years; during this time a stable lake area is established which can be compared with the present-day lake area. Superposed are random yearly fluctuations; climatic oscillations during the Holocene are not included since the magnitude and timing of these oscillations are not known for the study area and climate model simulations are absent. The paleoclimate for the Last Glacial Maximum has been derived from paleobotanical data from the Taymyr peninsula[32] by assuming a similar difference between present and past climate for both test areas.

ICEGROWTH : These experiments explore the effects of the growth rate of ground ice in the model on oscillatory behaviour of the system and thaw lake area. We varied the I_{grow} (volumetric ice growth rate) parameter between 0.001 and 0.005.

TIMING : These experiments are similar to TERRAIN, but with varying parameters for the M_P and M_T constants that relate the fraction of grid cells where thawing starts to precipitation and July temperature. The values of both parameters have been increased stepwise in value from 2.0e-6 to 1.0e-5. An experiment with the random creation of lakes with a prescribed total area (0.1 km^2) when a precipitation threshold is exceeded (300 mm) simulates the creation of lakes by flooding of terrain depressions by a precipitation surplus.

FUTURE : With these experiments we quantify future lake expansion as a result of Arctic climate warming by applying climate model simulation for the test area. We used climate model output from the following models: UK Met Office HadCM3 (HADCM3), Max Planck Institute for Meteorology ECHAM5 (ECHAM5), NOAA Geophysical Fluid Dynamics Laboratory CM2.1 (NOAAGFDL), CSIRO Atmospheric Research Mk3.5 (CSIRO), National Center for Atmospheric Research CCSM3.0 (NCAR) and Russian Institute for Numerical Mathematics INMCM3.0 (INMCM), each using the SRES A2 and B1 emission scenarios for the IPCC4th Assessment report (downloaded from
https://esg.llnl.gov:8443/home/publicHomePage.do
included in the World Climate Research Programme's (WCRP's) Coupled Model Intercomparison Project phase 3 (CMIP3) multi-model database[33]). The selected models show a similar range of climatic values as reported in the Arctic Climate Impact Assessment[34]. The

input climate time series were computed from monthly data from the climate model. The initial conditions for the lake area are generated by randomly creating circular lakes with a total area fraction of 0.08, which approximates the present lake area fraction of the IL area. The configuration of the drainage system is the same as for the TERRAIN experiment. For each of the climate model outputs, 10 runs of the thaw lake model have been produced, to capture the stochastic variability in the model output.

S 6. Experimental results.

The lake pattern generated by the model in the TERRAIN experiment and the terrain data have been compared using lake area fraction, lake size and isoperimetric quotient (ratio of the individual lake area and that of a circle having the same perimeter) indicating shape compactness (Table S4). Comparison of the model and terrain lake size distribution is hampered by uncertainty in the data; very small lakes in the terrain could not be digitized with sufficient accuracy due to the resolution of the remote sensing material, and some very large lakes could be included only partially in the digitized area. We determined the modeled lake areas and shapes by grid cell counting using the output of three model runs. The average lake area and number of lakes per km^2 does not deviate strongly from the observed values. The model generates a larger number of small lakes (one grid cell only) than is observed. Partly this can be attributed to the uncertainty in the digitized remote sensing material; higher resolution imagery of part of the area confirms a higher density of small lakes. The frequency distributions of the lake size and isoperimetric quotient for both model and field data are shown in Figure 2 of the article. The modeled lakes tend to be more compact than the observed lakes, in the study area a few lakes with a high isoperimetric quotient occur. With exception of the smallest modeled lakes, the modeled lake sizes and isoperimetric quotients arise from the same continuous distribution with the same median, as shown by a Mann-Whitney U test (Table S4).

Property	**Model-terrain comparison**	
	Model	*Terrain*
Number of lakes per km^2	0.36 ±0.01 (0.26 ±0.01)	0.31
Lake area fraction	0.083 ± 0.021 (0.081 ± 0.021)	0.099
Maximum thawed area fract.	0.242 ± 0.032	unknown
Average lake size km^2	0.230 (0.316)	0.310
Aver. isoperimetric quotient	2.34 ± 0.15	2.12
Test lake sizes	p=0.97, rank sum = 27955, z=0.04	
Test isoperimetric q.	p=0.10, rank sum = 38463, z=1.65	

Table S4. Statistical properties for the modelled and observed thaw lakes for the Kytalyk area. The model results are based on 3 model runs, the average and standard deviations for these runs are given. The numbers between brackets for the 'Model' column are calculated by excluding lakes consisting of only one grid cell. For testing of the size and shape (isoperimetric quotient) equality of model and data populations, the Mann-Whitney U test has been used with statistics listed in the table. The test for the lake size distribution excludes lakes consisting of only one grid cell (see text).

The areal distribution of the generated drained lake basins visually matches that of the IL area: smaller lake basins and remnants of the unthawed surface occur close to the river, and larger lake basins at distance from the river. This distribution results from the larger probability of lake drainage near the river, which strongly limits lake growth. The dominant wind direction is not clearly visible in both the modelled and terrain lakes; a larger wind direction factor F_w results in clearly oriented lakes however (not shown). Fig. S4 shows the effects of a different drainage density and an inhomogeneous ice distribution. A less dense drainage network causes the formation of a higher initial lake area peak and more pronounced oscillations since lakes can grow larger before drainage occurs. An inhomogeneous ground ice distribution affects the timing of the initial lake area peak, because areas with a lower ground ice volume hardly contribute to lake formation. Lake ages vary strongly but lakes may exist in the model for several thousands of years, in particular if located at some distance from the drainage lines, or when lake growth is retarded by low ice content in refrozen areas. The maximum lake expansion rate (L_{maxexp}) is on average 1.25 $m\ yr^{-1}$. Because of the effects of ground ice, the actual expansion rates (eq. 9) range between 0.38 and 1.0

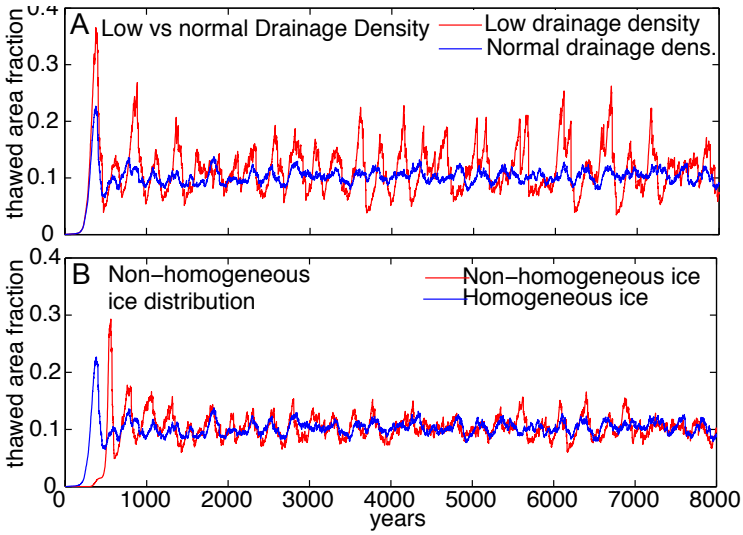

Figure S4. Effect of initial conditions on TERRAIN simulations. A: effect of a lower initial drainage densities. B: effect of an inhomogeneous ground ice distribution, with areas differing in average initial ground ice volume fraction.

$m\,yr^{-1}$. A video of the lake area evolution including 2500 model years of a sample model run is added as auxiliary material.

The timing of lake formation provides a second check on the model performance. Paleoclimate data in Siberia indicate that thaw lakes in the northern hemisphere started to form at 14-15 kyr BP and accelerated between 11.5-9 kyr BP, while the earliest recorded warming and precipitation increase occurred at ±13.6-14.7 kyr cal BP[23]. The major peak of thaw lake area appears to occur shortly after the rapid climate change of the LGT. The model reproduces a similar peak of lake formation, indicating that the model simulates the dynamics of the system correctly. In detail there are differences. Our model appears to reacts more slowly, which may have several causes. First, the radiocarbon database of LGT lake formation[23] may be biased towards older ages since lake sediments may contain older organic carbon. Second, we assume a simple step function of climate change, but preliminary warming and lake formation pre-dating the Bølling - Allerød interstadial may have occurred. The radiocarbon data show some thaw lake development around 18 kyr BP.[23], and in Western Europe widespread permafrost degradation occurred at the same time[35]. Third, model parameters may not have allowed sufficiently rapid lake formation and expansion. Fourth, our model includes

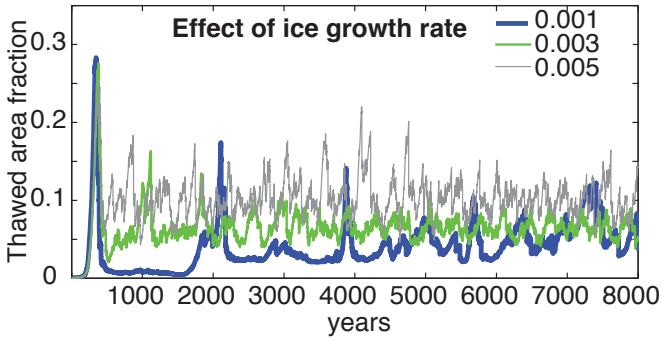

Figure S5. Effect of ice growth rate on oscillations in thaw lake area. Increasing the ice growth rate I_{grow} causes higher frequency and more regular oscillations, and a higher thaw lake area.

only one mode of lake formation (thaw pond formation at the most ice-rich sites), another mode may be filling of terrain depressions by precipitation increase[8].

The oscillations of the thaw lake area which are produced by the model after the initial lake area peak are an interesting feature. The radiocarbon database does not contradict oscillatory behavior[23]. Larger scale lake drainage, that may reduce lake area rapidly, also occurs in reality[17]. The length of the oscillations are affected by the ice regrowth factor I_{grow} (ICE-GROWTH experiment, Fig. S5). The lower the regrowth rate, the longer the oscillation period. With a larger ice growth rate the oscillations become shorter and less regular, and also the average lake area fraction increases. The oscillations become less regular and have a lower amplitude with time. Other parameters that affect the oscillations are M_P and M_T (higher values result in stronger oscillations) and drainage density (low drainage density results in stronger oscillations).

The TIMING experiments explore adjustments in the model to produce a faster response of lake formation. M_P and M_T are the constants that relate the fraction of grid cells where thawing starts to precipitation and summer temperature. In Figure S6 these have been increased in value from 2.0e-6 to 1.0e-5. This increase results in progressively earlier and more pronounced peaking of thaw lake area. With a value of 1.0e-5 for M_P and M_T the peak in thaw lake formation occurs shortly after the stepwise climate change, but the resulting lake configuration contains an unrealistically large number of very

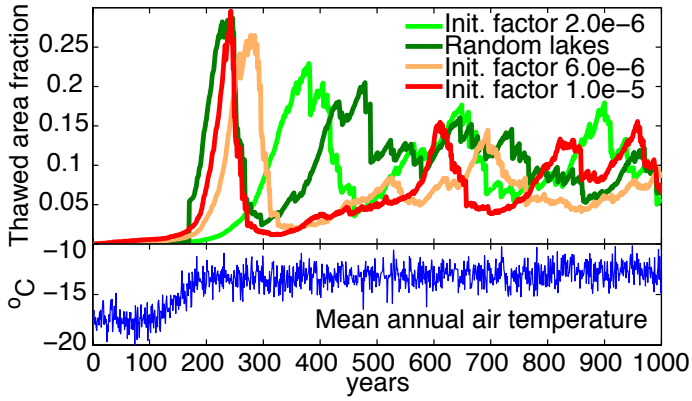

Figure S6. Effect of thaw lake initiation parameters on evolution of lake area. Increase of M_P and M_T moves the initial peak of thaw lake formation forward in time. Lake initiation by flooding of terrain depressions is simulated by generation of random lakes at a precipitation threshold of 300 mm. This also results in a thaw lake area peak immediately following climate change. Top: Thaw lake area evolution in time with different lake initiation parameters; below: mean annual air temperature for comparison.

small lakes, suggesting an unlikely high lake initiation rate. We therefore also simulated the creation of lakes by flooding of depressions, by generating lakes at random with a prescribed total area. This also results in a rapid lake expansion immediately after the climate change step without influencing the lake area distribution in the final results of the model.

For the FUTURE experiment, climate model output has been used (Figure S7). The simulated temperatures show an inter-model range of approximately 5 °C for the MAAT, 10 °C for July temperature and 150 mm for yearly precipitation. Several models start with a climate that deviates from the current climate in the study region, mostly with higher temperatures. The initial values of HADCM3 compare best with the current climate and therefore have been used for more detailed experiments described below.

The FUTURE experiments show for both the SRES A2 and B1 emission scenarios for most models a clear rise in the thawed area fraction (Figure 3). This rise is generated by expansion of existing lakes and to a smaller extent by creation of partially thawed grid cells. However, the increase of the

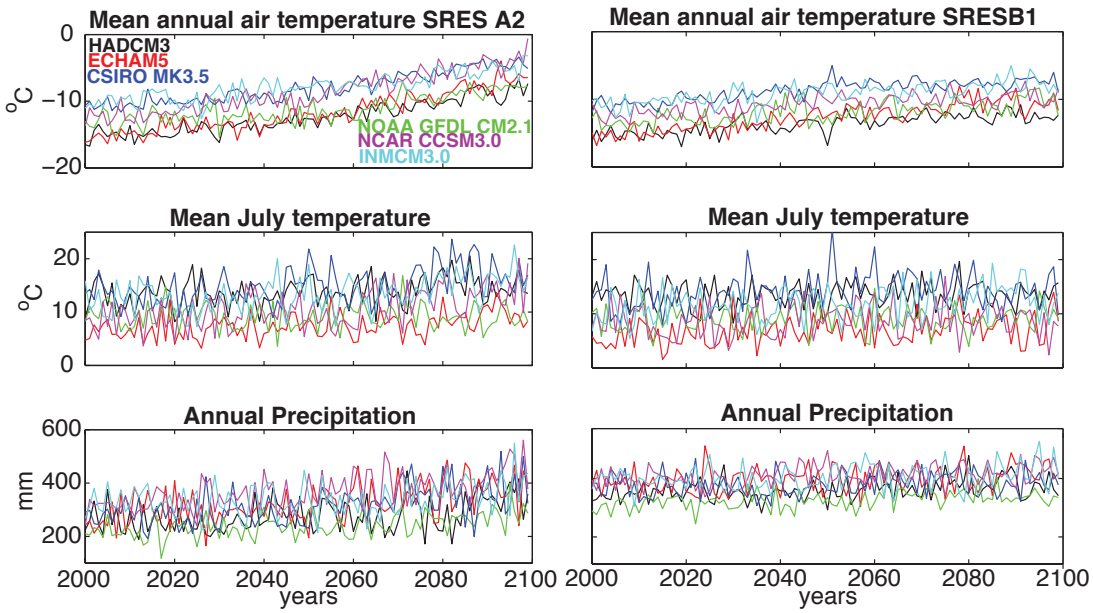

Figure S7. Climatic input for the FUTURE experiment. Mean annual air temperature (MAAT), mean July temperature and yearly precipitation for 2000 - 2099 from the climate models listed in S5. Left: simulations for the IPCC 4th Assessment SRES A2 scenario; right: B1 scenario.

thawed area fraction halts after approximately 50-70 years for most models, followed by a decrease caused by lake drainage. The turning point occurs somewhat later for the B1 scenario than for A2. Ultimately, most model runs result in a thawed area fraction which is even lower than the initial fraction. The thaw lake simulations for the various climate models differ mainly in the rate of decline of the thaw lake area. One exception are the runs driven by NOAAGFDL, which show a slower growth of the thawed area, and a decrease of the lake area which just starts at the end of the simulated century. This model combines low modeled MAAT and July temperatures with low precipitation. This combination results in low lake expansion rates and suppressed lake drainage (Figure S7, Figure 3). In all runs, the maximum lake expansion rate (L_{maxexp}) grows in the simulations from 1.2 to 2.2 $m\,yr^{-1}$ on average, but rates as high as 3.5 $m\,yr^{-1}$ occur. See eq. 9 for correction to the actual expansion rate $L_{i,j,t}$.

In the FUTURE experiments, we have included an experiment with smaller maximum ground ice volume fraction I_{max} (0.7 instead of 0.8). In this experiment (HADCM3 A2 climate), the lake area shrinks faster after reaching its maximum for $I_{max} = 0.7$ than for $I_{max} = 0.8$. At a low ice content the formation of new lakes occurs at a lower rate in the model, resulting in a relatively large effect of lake drainage (Figure S8). In a second experiment, we removed the dependency of lake expansion on precipitation, by setting the c constant in eq. 7 to 0. This resulted in a similar pattern as in the model runs based on the NOAAGFDL model: slower increase of thawed area (not shown).

S 7. CH_4 emission estimates.

Estimates of the area that is susceptible to thaw lake development differ. The entire area of ice-rich 'yedoma' sediments, which are susceptible to thaw lake formation, is estimated at 10^6 km^2 [36,37,38]. The circumpolar permafrost map[39] contains 0.94×10^6 km^2 of continuous permafrost with high to medium ice content, which should be sensitive to lake development. High-medium ice content discontinuous permafrost accounts for another 0.18×10^6 km^2, but in these areas drainage through taliks is more likely[37]. For the LGT also permafrost areas that are presently below sealevel due to sealevel rise should be included[40,23]; the total LGT yedoma area is estimated at 1.9×10^6 km^2.

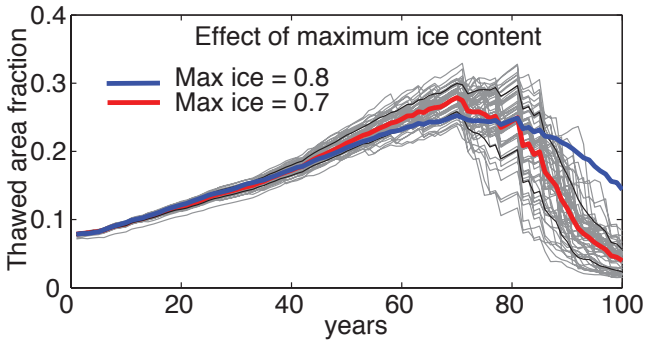

Figure S8. Effect of maximum ice content on FUTURE simulations. Decreasing the maximum volumetric ground ice fraction to 0.7 results in a stronger effect of lake drainage because less new lakes are formed (average lake area: red line, standard deviations: black lines, individual simulations: grey lines). Climate: HadCM3 A2 scenario. For comparison the average of the simulations of Figure 3 is shown.

CH_4 emission from North Siberian thaw lakes amounts 25 ± 5 g CH_4 m^{-2} yr^{-1} based on an intensive survey of three lakes[41]. To quantify the CH_4 emission added by lake development for the present-day environment, the emission of non-lake tundra that should have occurred otherwise should be subtracted. For the test area, this is quantified by chamber flux measurements between the years 2003 and 2006 (±4.1 g CH_4 m^{-2} yr^{-1})[26,27], confirmed recently with eddy covariance measurements and modelling over the summer seasons of 2007-2009[42]. This results in a net emission increase of 20.9 ± 5 g CH_4 m^{-2} yr^{-1} for a change from tundra to lake. On a continuous permafrost site with wet tundra in northern Greenland, high emissions have been observed in autumn during soil freezing, which may approximate the summer emissions in magnitude[43]. If this also occurs in the Siberian tundra (which is speculative until proper quantification) this would further decrease the calculated emissions attributed to lake emission. For the conversion of drier[25,32] LGT environments to lakes we assume a non-emitting land surface.

The TERRAIN simulations result in an average maximum of the lake area fraction of 0.248±0.026. At this maximum, the CH_4 emission in the model area should have been increased with 6.2±0.2 g CH_4 m^{-2} yr^{-1} for the test area due to lake formation. Extrapolating over the entire ice-rich 'yedoma' area at the LGT this results in a peak emission of 11.78±0.28 Tg CH_4 yr^{-1}. Integrating over the entire initial thaw lake peak lasting from 100

till 470 years and the model grid of 400 km^2, the emission is 0.288 Tg CH_4. Again extrapolating over the entire LGT yedoma this would result in a total emission of 1368±44 Tg CH_4 due to lake formation, over 370 years of the peak duration, or 3.73 Tg CH_4 yr^{-1}.

In a similar fashion, future emissions resulting from arctic climate change can be based on the FUTURE model experiments, taking into account terrestrial tundra wetland emissions. We used an average of 50 simulations based on the HADCM3 climate model, which shows for the first 10 years a good agreement with the present climate in the study region (note that the simulations for other climate models differ in the decline of the thaw lake area, Figure 3). The average lake area results in an average increase of the thawed area fraction of 0.08 to a maximum 0.25±0.03 after 70 years for the A2 scenario and 0.25±0.03 after 71 years for B1. Applying the net emission factor for tundra-lake conversion above, the maximal emission increase is 3.49±0.52 g CH_4 m^{-2} yr^{-1} for the A2 scenario, 3.53±0.55 g CH_4 m^{-2} yr^{-1} for the B1 scenario. Integrating over the 100 model years the lake area is larger by a fraction of 0.094±0.002 for A2 and 0.098±0.002 for B1, resulting in an emission increase of 1.96±0.05 g CH_4 m^{-2} yr^{-1} and 2.05±0.05 g CH_4 m^{-2} yr^{-1} respectively. Assuming that our test area can be extrapolated over the entire present-day ice-rich continuous permafrost area, 0.94×10^6 km^2, the maximum emission would be 3.28±0.49 Tg CH_4 yr^{-1} and the average over 100 years 1.84±0.04 Tg CH_4 yr^{-1} for A2, and respectively 3.32±0.52 Tg CH_4 yr^{-1} and 1.92±0.04 Tg CH_4 yr^{-1} for B1. The amount of ground ice volume assumed does not have large effect; if we reduce the maximum ground ice volume as in the ground ice sensitivity experiment of FUTURE, the averaged yearly emission for A2 would be 1.71±0.02 Tg CH_4 yr^{-1} (Fig. S8). We have restricted our calculation to continuous permafrost since our model does not yet include underground drainage of lakes through taliks; if discontinuous high ice content permafrost is included, the emissions are at most 19% higher.

An important restriction on the effect of lake drainage on CH_4 emission is the type of ecosystem that result from drainage. Observations in the low relief test area show that river-connected lakes are usually not completely drained, but obtain a water level that fluctuates strongly with river water level and ultimately may be filled with sediment. In the higher relief area just south of the test area, complete drainage is more common. The wetland areas that remain after lake drainage may have relatively high CH_4 emission, although their carbon sequestration rates also may be high[27].

References

[1] Hopkins, D. M. Thaw lakes and thaw sinks in the Imuruk Lake area, Seward Peninsula. *J. Geol.* **57**, 119131 (1949).

[2] Brouchkov, A., Fukuda, M., Fedorov, A., Konstantinov, P., Iwahana, G. Thermokarst as a short-term permafrost disturbance, Central Yakutia. *Permafr. Perigl. Processes* **15**, 8187 (2004).

[3] Billings, W. D., and Peterson, K. M. Vegetational change and ice-wedge polygons through the thaw-lake cycle in arctic Alaska. *Arctic and Alpine Res.* **12**, 413432 (1980).

[4] Hinkel, K.M., Hurd, J.K. Jr. Permafrost destabilization and thermokarst following snow Fence Installation, Barrow, Alaska, U.S.A. *Arctic Antarctic Alpine Res.* **38**, 530539 (2006).

[5] Fedorov, A.N., Konstantinov, P.Y. Response of permafrost landscapes of Central Yakutia to current changes of climate, and anthropogenic impacts. *Geogr. Nat. Resources* **30**, 146150 (2009).

[6] Jorgenson, M.T., Shur, Y.L., Pullman, E.R. Abrupt increase in permafrost degradation in Arctic Alaska. *Geophys. Res. Letters* **33**, L02503, doi:10.1029/2005GL024960 (2006).

[7] Iijima, Y., Fedorov., A.N., Park., H., Suzuki, K., Yabuki, H., Maximov, T.C., Ohata, T. Abrupt increases in soil temperature following increased precipitation in a permafrost region, Central Lena river basin, Russia. *Permafr. Perigl. Processes* **21**, 30-41 (2010).

[8] Jorgenson,M.T., Shur, Y.L. Evolution of lakes and basins in northern Alaska and discussion of the thaw lake cycle. *J. Geophys. Res.* **112**, F02S17, doi:10.1029/2006JF000531 (2007).

[9] Hinkel, K.M., Eisner, W.R., Bockheim, J.G., Nelson, F.E., Peterson, K.M., Dai, X. Spatial Extent, Age, and Carbon Stocks in Drained Thaw Lake Basins on the Barrow Peninsula, Alaska. *Arctic Antarctic Alpine Res.* **35**, 291300 (2003).

[10] Ling, F., Zhang, T. Numerical simulation of permafrost thermal regime and talik development under shallow thaw lakes on the

Alaskan Arctic Coastal Plain. *J. Geophys. Res.* **108**, D16, 4511, doi:10.1029/2002JD003014 (2003).

[11] Pelletier, J. Formation of oriented thaw lakes by thaw slumping. *J. Geophys. Res.* **110**, F02018, doi:10.1029/2004JF000158 (2005).

[12] Hinkel, K.M., Jones, B.M., Eisner, W.R., Cuomo, C.J., Beck, R.A., Frohn, R. Methods to assess natural and anthropogenic thaw lake drainage on the western Arctic coastal plain of northern Alaska. *J. Geophys. Res.* **112**, F02S16, doi:10.1029/2006JF000584 (2007)

[13] West, J.J., Plug, L.J. Time-dependent morphology of thaw lakes and taliks in deep and shallow ground ice. *J. Geophys. Res.* **113**, F01009, doi:10.1029/2006JF000696 (2008).

[14] Hinkel, K.M., Frohn, R.C, Nelson, F.E., Eisner, W.R., Beck, R.A. Morphometric and spatial analysis of thaw lakes and drained thaw lake basins in the Western Arctic Coastal Plain, Alaska. *Permafr. Perigl. Processes* **16**, 327341 (2005).

[15] Plug, L.J., Scott, B.M., Walls, C. Thermokarst lake changes from 19782001 on the Tuktoyaktuk Peninsula, Western Canadian Arctic *Geophys. Res.Lett.* **35**, L03502, doi:10.1029/2007GL032303 (2006).

[16] Smith, L.C., Sheng, Y., MacDonald, G.M., Hinzman, L.D. Disappearing Arctic lakes. *Science* **308**, 1429 doi:10.1126/science.1108142 (2005).

[17] Mackay, J.R. Catastrophic lake drainage, Tuktoyaktuk Peninsula area, District of Mackenzie. *Current Research, Part D, Geol. Surv. Canada* **88-1D**, 8390 (1988).

[18] Katamura, F., Fukuda, M., Bosikov, N.P., Desyatkin, R.V., Nakamura, T., Moriizumi, J.. Thermokarst formation and vegetation dynamics inferred from a palynological study in Central Yakutia, Eastern Siberia, Russia. *Arctic Antarctic Alpine Res.* **38**, 561570 (2006).

[19] Van Huissteden, J. Tundra rivers of the Last Glacial: sedimentation and geomorphological processes during the Middle Pleniglacial in the Dinkel valley (eastern Netherlands). *Meded.Rijks Geol. Dienst* **44**, 3-138 (1990)

[20] Marsh, P., Russell, M., Pohl, S., Haywood, H., Onclin, C. Changes in thaw lake drainage in the Western Canadian Arctic from 1950 to 2000. *Hydrol. Process.* **23**, 145158 (2009).

[21] Mackay, J.R., Burn C.R. The first 20 years (19781979 to 1998 1999) of active-layer development, Illisarvik experimental drained lake site, western Arctic coast. Canada, *Can. J. Earth Sci.* **39**, 1657 1674 (2002).

[22] Billings, W. D., and Peterson, K. M. Vegetational change and ice-wedge polygons through the thaw-lake cycle in arctic Alaska. *Arctic and Alpine Res.* **12**, 413432 (1980).

[23] Walter, K.M., Edwards, M.E., Grosse, G., Zimov, S.A., Chapin III F.S. Thermokarst lakes as a source of atmospheric CH_4 during the Last Deglaciation. *Science* **318**, 633-636 (2007).

[24] Plug, L.J, West, J.J. Thaw lake expansion in a two-dimensional coupled model of heat transfer, thaw subsidence, and mass movement. *J. Geophys. Res.* **114**, F01002, doi:10.1029/2006JF000740 (2009).

[25] Schirrmeister, L., Kunitsky, V., Grosse G., Wetterich, S., Meyer, H., Schwamborn, G., Babiy, O., Derevyagin, A., Siegert, C. Sedimentary characteristics and origin of the Late Pleistocene Ice Complex on northeast Siberian Arctic coastal lowlands and islands - A review. *Quat. Intern.* doi:10.1016/j.quaint.2010.04.004 (2010).

[26] Van Huissteden J., Maximov, T.C., Kononov, A.V., Dolman, A.J. High methane flux from an arctic floodplain (Indigirka lowlands, eastern Siberia). *J. Geophys. Res.* **110**, G02002, doi:10.1029/2005JG000010 (2005).

[27] Van der Molen, M.K., Van Huissteden, J., Parmentier, F.J.W., Petrescu, A.M.R., Dolman, A.J., Maximov, T.C., Kononov, A.V., Karsanaev, S.V., Suzdalov, D.A. The growing season greenhouse gas balance of a continental tundra site in the Indigirka lowlands, NE Siberia. *Biogeosciences* **4**, 9851003 (2007)

[28] Pavlov, A.V. Permafrost-climatic monitoring of Russia: Analysis of field data and forecast. *Polar Geography* **31**, 27-46 (2008).

[29] Perk, A.A., Chevychelov, A.P., Skrybykina, V.P. Climatic characteristic of growing season in Central Yakutia over the last 65 years. In: Maximov, T.C., Ohta, T., Dolman, A.J., Moors, E., Ohata, T. (Eds): *Proceedings of the the international semi-open workshop C/H2O/Energy Balance and Climate over Boreal regions with special emphasis on Eastern Eurasia'*, p. 109-112 (2004).

[30] Van Huissteden, J., Vandenberghe, J., D. Pollard D.: Palaeotemperature reconstructions of the European permafrost zone during Oxygen Isotope Stage 3 compared with climate model results. *J. Quat. Sci.* **18**, 453-464 (2003).

[31] French, H.M. *The Periglacial environment*. Longman, 341 pp (1996).

[32] Andreev, A.A.. Tarasov, P.E., Siegert, C., Ebel, T., Klimanov, V.A., Melles, M., Bobrov, A.A., Dereviagin, A.Y., Lubinski, D.J., Hubberten, H.-W. Late Pleistocene and Holocene vegetation and climate on the northern Taymyr Peninsula, Arctic Russia. *Boreas* **32**, 484505 (2003).

[33] Meehl, G. A., C. Covey, T. Delworth, M. Latif, B. McAvaney, J. F. B. Mitchell, R. J. Stouffer, and K. E. Taylor, 2007: The WCRP CMIP3 multi-model dataset: A new era in climate change research. *Bull. Am. Meteorol. Soc.* **88**, 1383-1394.

[34] ACIA. *Arctic Climate Impact Assessment.* Cambridge University Press, 1042p (2005).

[35] Bateman, M.D., Van Huissteden, J. The timing of last-glacial periglacial and aeolian events, Twente, eastern Netherlands. *J. Quat. Sci.* **14**, 277283 (1999).

[36] Walter, K.M., Zimov, S.A., Chanton, J.P., Verbyla, D., Chapin, F.S.III. Methane bubbling from Siberian thaw lakes as positive feedback to climate warming. *Nature* **443**, doi: 10.1038/nature 05040 (2006).

[37] Walter, K.M., Smith, L.C., Chapin, F.S.III. Methane bubbling from northern lakes: present and future contributions to the global methane budget. *Phil. Trans. R. Soc.* **A 365**, 16571676 (2007).

[38] Zimov, S.A., Davydov, S.P. Zimova, G.M. Davydova, A.I. Schuur, E.A.G. Dutta, K., Chapin III, F.S. Permafrost carbon: Stock and decomposability of a globally significant carbon pool. *Geophys. Res. L.* **33**, L20502, doi:10.1029/2006GL027484 (2006).

[39] Brown, J., O.J. Ferrians Jr., J.A. Heginbottom, and E.S. Melnikov. *Circum-Arctic map of permafrost and ground-ice conditions*. Boulder, CO: National Snow and Ice Data Center/World Data Center for Glaciology. Digital Media (2001).

[40] Van Huissteden, J. Methane emission from northern wetlands in Europe during Oxygen Isotope Stage 3. *Quat. Sci. Rev.* **23**, 1989-2005 (2004)

[41] Walter Anthony, K.M., Vas, D.A., Brosius, L., Stuart Chapin III, F., Zimov, S.A., Zhuang, Q. Estimating methane emission from northern lakes using ice-bubble surveys. *Limnology and Oceanography: Methods* **8**, 592609 (2010).

[42] Parmentier, F.J.W., Van Huissteden, J., Van der Molen, M.K., Dolman, A.J., Karsanaev, S.A., Maximov, T.C. Spatial and temporal dynamics in eddy covariance observations of methane fluxes at a tundra site in Northeastern Siberia. Submitted to *J. Geophys. Res.*

[43] Mastepanov N., Sigsgaard, C., Dlugokencky, E.J., Houweling, S., Strom, L., Tamstorf, M.P., Christensen, T.R. Large tundra methane burst during onset of freezing. *Nature* **456** 628-631